Instrumental Neutron Activation Analysis of Inka Pottery from Chile, Northwest Argentina, and Bolivia

Report Prepared by:
Robert J. Speakman and Michael D. Glascock
Archaeometry Laboratory
Missouri University Research Reactor
University of Missouri
Columbia, MO 65211

For:
Dra. Veronica Williams
Inst Ciencias Antropologicas
Condarco 55 Piso 12
Dpto C Wilde
Prov Bs As
1875

veronicaw33@yahoo.com

December 14, 2005

Introduction

Dra. Williams is investigating Inka economy in the southern Andes through examination of the production and distribution of ceramics used in state-controlled activities. It constitutes one step of a long-term, collaborative international project on the Inka Empire, conducted by scholars from the United States and Argentina. In broadest terms, the research is intended to provide insight into the political and economic considerations that underwrote the economy of the largest and arguably most complex polity formed in the prehispanic New World. Toward this end, instrumental neutron activation analysis (INAA) has been undertaken on 459 pottery (n = 414) and clay samples (n = 45) from Inka provinces in northwest Argentina (in the modern Salta, Jujuy, and Catamarca provinces), Northern Chile, and the Bolivian Altiplano. The analyses were conducted at the University of Missouri Research Reactor Center (MURR). Here we describe sample preparation and analytical techniques used at MURR and report on the subgroup structure discovered in the chemical data.

Sample Preparation

Pottery samples were prepared for INAA using procedures standard at MURR. Fragments of about $1cm^2$ were removed from each sample and abraded using a silicon carbide burr in order to remove glaze, slip, paint, and adhering soil, thereby reducing the risk of measuring contamination. The samples were washed in deionized water and allowed to dry in the laboratory. Once dry, the individual sherds were ground to powder in an agate mortar to homogenize the samples. Archival samples were retained from each sherd (when possible) for future research.

Clay samples were fired in a furnace to 700 degrees Celsius for one hour. A portion of each clay was then ground to powder in an agate mortar to homogenize the samples. A fired archival sample was retained from each clay (when possible) for future research. Unfired clays were destroyed per USDA requirements.

Two analytical samples were prepared from each source specimen. Portions of approximately 150 mg of powder were weighed into clean high-density polyethylene vials used for short irradiations at MURR. At the same time, 200 mg of each sample was weighed into clean high-purity quartz vials used for long irradiations. Individual sample weights were recorded to the nearest 0.01 mg using an analytical balance. Both vials were sealed prior to irradiation. Along with the unknown samples, Standards made from National Institute of Standards and Technology (NIST) certified standard reference materials of SRM-1633a (coal fly ash) and SRM-688 (basalt rock) were similarly prepared, as were quality control samples (e.g., standards treated as unknowns) of SRM-278 (obsidian rock) and Ohio Red Clay (a standard developed for in-house applications).

Irradiation and Gamma-Ray Spectroscopy

Neutron activation analysis of ceramics at MURR, which consists of two irradiations and a total of three gamma counts, constitutes a superset of the procedures used at most other NAA laboratories (Glascock 1992; Neff 1992, 2000). As discussed in detail by Glascock (1992), a short irradiation is carried out through the pneumatic tube irradiation system. Samples in the polyvials are sequentially irradiated, two at a time, for five seconds by a neutron flux of 8×10^{13} n cm^{-2} s^{-1} The 720-second count yields gamma spectra containing peaks for nine short-lived

elements aluminum (Al), barium (Ba), calcium (Ca), dysprosium (Dy), potassium (K), manganese (Mn), sodium (Na), titanium (Ti), and vanadium (V). The samples are encapsulated in quartz vials and are subjected to a 24–hour irradiation at a neutron flux of 5 x 10^{13} n cm^{-2} s^{-1}. This long irradiation is analogous to the single irradiation utilized at most other laboratories. After the long irradiation, samples decay for seven days, and then are counted for 1,800 seconds (the "middle count") on a high-resolution germanium detector coupled to an automatic sample changer. The middle count yields determinations of seven medium half-life elements, namely arsenic (As), lanthanum (La), lutetium (Lu), neodymium (Nd), samarium (Sm), uranium (U), and ytterbium (Yb). After an additional three- or four-week decay, a final count of 8,500 seconds is carried out on each sample. The latter measurement yields the following 17 long half-life elements: cerium (Ce), cobalt (Co), chromium (Cr), cesium (Cs), europium (Eu), iron (Fe), hafnium (Hf), nickel (Ni), rubidium (Rb), antimony (Sb), scandium (Sc), strontium (Sr), tantalum (Ta), terbium (Tb), thorium (Th), zinc (Zn), and zirconium (Zr).

The element concentration data from the three measurements are tabulated in parts per million using the EXCEL spreadsheet program. Descriptive data for the archaeological samples are appended to the concentration spreadsheet and the data are also stored in a dBASE/FOXPRO database file useful for organizing, sorting, and extracting sample information. The data file enclosed with this report contains the sample database in EXCEL format.

Interpreting Chemical Data

The analyses at MURR described previously produced elemental concentration values for 32 or 33 elements in most of the analyzed samples. Data for Ni in most samples was below detection limits (as is the norm for most New World ceramic analyses) and was removed from consideration during the statistical analysis. In addition As, Nd, U, and Tb have higher counting errors. In order to minimize variation within the dataset, these elements were removed from consideration. Statistical analysis was subsequently carried out on base-10 logarithms of concentrations on the remaining 28 elements. Use of log concentrations rather than raw data compensates for differences in magnitude between the major elements, such as calcium, on one hand and trace elements, such as the rare earth or lanthanide elements (REEs). Transformation to base-10 logarithms also yields a more normal distribution for many trace elements.

The interpretation of compositional data obtained from the analysis of archaeological materials is discussed in detail elsewhere (e.g., Baxter and Buck 2000; Bieber et al. 1975; Bishop and Neff 1989; Glascock 1992; Harbottle 1976; Neff 2000) and will only be summarized here. The main goal of data analysis is to identify distinct homogeneous groups within the analytical database. Based on the provenance postulate of Weigand *et al*. (1977), different chemical groups may be assumed to represent geographically restricted sources. For lithic materials such as obsidian, basalt, and cryptocrystalline silicates (e.g., chert, flint, or jasper), raw material samples are frequently collected from known outcrops or secondary deposits and the compositional data obtained on the samples is used to define the source localities or boundaries. The locations of sources can also be inferred by comparing unknown specimens (i.e., ceramic artifacts) to knowns (i.e., clay samples) or by indirect methods such as the “criterion of abundance” (Bishop *et al.* 1992) or by arguments based on geological and sedimentological characteristics (e.g., Steponaitis *et al.* 1996). The ubiquity of ceramic raw materials usually makes it impossible to sample all

potential “sources” intensively enough to create groups of knowns to which unknowns can be compared. Lithic sources tend to be more localized and compositionally homogeneous in the case of obsidian or compositionally heterogeneous as is the case for most cherts.

Compositional groups can be viewed as “centers of mass” in the compositional hyperspace described by the measured elemental data. Groups are characterized by the locations of their centroids and the unique relationships (i.e., correlations) between the elements. Decisions about whether to assign a specimen to a particular compositional group are based on the overall probability that the measured concentrations for the specimen could have been obtained from that group.

Initial hypotheses about source-related subgroups in the compositional data can be derived from non-compositional information (e.g., archaeological context, decorative attributes, etc.) or from application of various pattern-recognition techniques to the multivariate chemical data. Some of the pattern recognition techniques that have been used to investigate archaeological data sets are cluster analysis (CA), principal components analysis (PCA), and discriminant analysis (DA). Each of the techniques has it own advantages and disadvantages which may depend upon the types and quantity of data available for interpretation.

The variables (measured elements) in archaeological and geological data sets are often correlated and frequently large in number. This makes handling and interpretation patterns within the data difficult. Therefore, it is often very useful to transform the original variables in the data set into a smaller set of uncorrelated variables in order to make data interpretation easier. Of the above-mentioned pattern recognition techniques, PCA is a technique that transforms from the data from the original correlated variables into uncorrelated variables most easily.

PCA creates a new set of reference axes arranged in decreasing order of variance subsumed. The individual PCs are linear combinations of the original variables. The data can be displayed on combinations of the new axes, just as they can be displayed on the original elemental concentration axes. PCA can be used in a pure pattern-recognition mode, i.e., to search for subgroups in an undifferentiated data set, or in a more evaluative mode, i.e., to assess the coherence of hypothetical groups suggested by other criteria. Generally, compositional differences between specimens can be expected to be larger for specimens in different groups than for specimens in the same group, and this implies that groups should be detectable as distinct areas of high point density on plots of the first few components.

It is well known that PCA of chemical data is scale dependent (Mardia *et al*. 1979), and analyses tend to be dominated by those elements or isotopes for which the concentrations are relatively large. As a result, standardization methods are common to most statistical packages. A common approach it to transform the data into logarithms (to base 10). As an initial step in the PCA of most chemical data at MURR, the data are transformed into log concentrations to equalize the differences in variance between the major elements such as Al, Ca and Fe, on one hand and trace elements, such as the rare-earth elements (REEs), on the other hand. An additional advantage of the transformation is that it appears to produce more nearly normal distributions for the trace elements.

One frequently exploited strength of PCA, discussed by Baxter (1992), Baxter and Buck (2002), and Neff (1994, 2002), is that it can be applied as a simultaneous R- and Q-mode technique, with both variables (elements) and objects (individual analyzed samples) displayed on the same set of principal component reference axes. A plot using the first two principal components as axes is usually the best possible two-dimensional representation of the correlation or variance-covariance structure within the data set. Small angles between the vectors from the origin to variable coordinates indicate strong positive correlation; angles at 90 degrees indicate no correlation; and angles close to 180 degrees indicate strong negative correlation. Likewise, a plot of sample coordinates on these same axes will be the best two-dimensional representation of Euclidean relations among the samples in log-concentration space (if the PCA was based on the variance-covariance matrix) or standardized log-concentration space (if the PCA was base on the correlation matrix). Displaying both objects and variables on the same plot makes it possible to observe the contributions of specific elements to group separation and to the distinctive shapes of the various groups. Such a plot is commonly referred to as a "biplot" in reference to the simultaneous plotting of objects and variables. The variable inter-relationships inferred from a biplot can be verified directly by inspecting bivariate elemental concentration plots. [Note that a bivariate plot of elemental concentrations is not a biplot.]

Whether a group can be discriminated easily from other groups can be evaluated visually in two dimensions or statistically in multiple dimensions. A metric known as the Mahalanobis distance (or generalized distance) makes it possible to describe the separation between groups or between individual samples and groups on multiple dimensions. The Mahalanobis distance of a specimen from a group centroid (Bieber *et al*. 1976, Bishop and Neff 1989) is defined by:

$$D^2_{y,X} = [y - \overline{X}]^t I_x [y - \overline{X}]$$

where y is the 1 x m array of logged elemental concentrations for the specimen of interest, X is the n x m data matrix of logged concentrations for the group to which the point is being compared with $\overline{X}$ being it 1 x m centroid, and I_x is the inverse of the m x m variance-covariance matrix of group X. Because Mahalanobis distance takes into account variances and covariances in the multivariate group it is analogous to expressing distance from a univariate mean in standard deviation units. Like standard deviation units, Mahalanobis distances can be converted into probabilities of group membership for individual specimens. For relatively small sample sizes, it is appropriate to base probabilities on Hotelling's T^2, which is the multivariate extension of the univariate Student's t.

When group sizes are small, Mahalanobis distance-based probabilities can fluctuate dramatically depending upon whether or not each specimen is assumed to be a member of the group to which it is being compared. Harbottle (1976) calls this phenomenon "stretchability" in reference to the tendency of an included specimen to stretch the group in the direction of its own location in elemental concentration space. This problem can be circumvented by cross-validation, that is, by removing each specimen from its presumed group before calculating its

own probability of membership (Baxter 1994; Leese and Main 1994). This is a conservative approach to group evaluation that may sometimes exclude true group members.

Small sample and group sizes place further constraints on the use of Mahalanobis distance: with more elements than samples, the group variance-covariance matrix is singular thus rendering calculation of I_x (and D^2 itself) impossible. Therefore, dimensionality of the groups must somehow be reduced. One approach would be to eliminate elements considered irrelevant or redundant. The problem with this approach is that the investigator's preconceptions about which elements should be discriminate may not be valid. It also squanders the main advantage of multielement analysis, namely the capability to measure a large number of elements. An alternative approach is to calculate Mahalanobis distances with the scores on principal components extracted from the variance-covariance or correlation matrix for the complete data set. This approach entails only the assumption, entirely reasonable in light of the above discussion of PCA, that most group-separating differences should be visible on the first several PCs. Unless a data set is extremely complex, containing numerous distinct groups, using enough components to subsume 90% of the total variance in the data can be generally assumed to yield Mahalanobis distances that approximate Mahalanobis distances in full elemental concentration space.

Lastly, Mahalanobis distance calculations are also quite useful for handling missing data (Sayre 1975). When many specimens are analyzed for a large number of elements, it is almost certain that a few element concentrations will be missed for some of the specimens. This occurs most frequently when the concentration for an element is near the detection limit. Rather than eliminate the specimen or the element from consideration, it is possible to substitute a missing value by replacing it with a value that minimizes the Mahalanobis distance for the specimen from the group centroid. Thus, those few specimens which are missing a single concentration value can still be used in group calculations.

Results and Conclusion

Analysis of the data resulted in the identification of 11 compositional groups: Groups 1–9, and Groups X and Y. One hundred and twenty-one pottery samples (ca. 30% of the analyzed pottery samples) are unassigned. In the current study, specimens were left unassigned if they were marginal to all groups (e.g., less than 1% probability of membership), if they showed compositional affiliations with more than one group (high probabilities in multiple groups), or if including a specimen in the group to which it apparently belonged obscured distinctions between groups that were otherwise well discriminated. In most cases, the unassigned samples have less than 1% probability in any of the groups, or they exceed more than 1% probability of membership in one or more groups. Although unassigned specimens are problematic, the approach taken herein is similar to that taken by most INAA laboratories and serves to minimize incorrect group assignments by leaving marginal specimens unassigned (Neff et al. 2006). It is probable that future analyses of pottery from Northwest Argentina will facilitate the identification additional compositional groups thereby enabling many of these samples to be assigned to a compositional group.

The complete subgroup structure in Inka dataset is documented in fourteen figures

included at the end of this report. Seven tables, raw data, and descriptive information are included in the Excel file accompanying this report.

Table 1 lists the analyzed specimens and compositional affiliations determined in the present investigation together with descriptive information and data in parts-per-million (ppm).

Table 2 lists Mahalanobis distance-based probabilities of membership in the largest groups (1, 2, 3, 4, 5, 6, 9, X); these probabilities are based on principal components 1–14 analysis which accounts for more than 94% of the cumulative variation in the dataset (see Table 7). All specimens are "jackknifed," as discussed above. A 1% cut-off was used in determining group assignments. Samples generally exceed 1% probability of membership in the group to which they are assigned and have less than 1% probability of membership in the other groups.

Table 3 lists probabilities of group membership for the smaller groups (6, 7, 8, Y) and the unassigned samples. With smaller groups it is not possible to calculate Mahalanobis distance probabilities of group membership. However, the validity of these groups can be assessed by projecting smaller groups against the larger groups. In an ideal situation samples assigned to smaller groups will have less than 1% probability of membership in the larger groups—as is the case herein. A few unassigned samples exceed 1% probability of membership in Group 4 or Group-X. However, these groups are relatively heterogeneous, and including these samples in one or the other of these groups only blur distinction between groups that were otherwise well-separated.

Table 4 is a cross tabulation of compositional group by ceramic type.

Table 5 is a cross tabulation of compositional group by archaeological site.

Table 6 lists probabilities of group membership for clays.

Table 7 lists the eigenvectors and eigenvalues derived from PCA of the dataset. Table 7 also explains the percentage of cumulative variance within the dataset.

A PCA biplot based on the correlation matrix of the complete data set is shown in Figures 1–4. As explained above, the PCA biplot affords a means for assessing the contributions of various elements to the identified subgroup structure. PCA resulted in the identification of four large groups and one smaller group. Interestingly, these groups correspond to broad geographic zones—Titicaca Basin (Group-1), Northern Chile (Group-2), Northwest Argentina, and an unknown area (Groups X and Y). A similar pattern can be seen in Figure 5, a plot of samarium and europium concentrations.

Group 1 (n = 18) is assumed to represent pottery produced in the *Titicaca basin* based on the fact that 9 of the 15 (Table 5) analyzed samples from Titicaca are assigned to Group-1. Of

the remaining 9 samples assigned to this group, seven are from northern Chilean archaeological contexts and one was recovered from a site in Salta Province. Comparison of Group-1 with D'Altroy's Mantaro Valley and Titicaca basin samples (analyzed at BNL) provides further support that Group-1 pottery originates from the Titicaca basin.

Group 2 (n=48) is comprised almost exclusively of pottery recovered from sites in Northern Chile. Because this group includes pottery from so many sites, it is probable that may subsume multiple compositional groups. Additional sampling will aid in evaluating the homogeneity of this group. Currently, the most conservative approach is to treat this as a single group until additional analyses from Northern Chile become available.

Group X is a unique group of 20 samples from Potrero-Chaquiago in Catamarca. Intuitively, it would seem that Group X is derived from Potrero-Chaquiago. However, given that the compositional profile of this group is so different from most of the other pottery analyzed, it is more likely that this pottery was imported to Potrero-Chaquiago from an unknown production area. Interestingly, 35% of the pottery assigned to this group is classified as Cusco polychrome raising the possibility that this group may represent pottery production in Southern Peru.

Group Y is similar to Group X in that it exhibits an unusual compositional profile (relative to the Inka database). The four samples assigned to this group are from sites located in Catamarca and three of the samples are classified as Cusco polychrome.

Finally, the bulk of the analyzed sample forms a large macro-group we have designated **Northwest Argentina**. This group represents pottery production in Northwest Argentina, and can be further subdivided into seven groups (Groups 3–9, Figures 6–12). Figure 6 is a biplot based on PCA of the Northwest Argentina pottery. This plot shows relatively good separation of the seven pottery groups. Better separation of Groups 5, 8, and, 9 are shown in Figures 8 and 9. Likewise, better separation of groups 4 and 7 is shown in Figure 10. In addition to the PCA and elemental plots, discriminant analysis also can be used to illustrate the differences between the groups (Figures 11 and 12). It is important to stress however that discriminant analysis is only used as an illustrative tool, and was not used in assigning samples to the various groups.

Group 3 is comprised entirely of Yocavil Polychrome and Famabalasto Black-on-red pottery (Table 4) and more than 80% of the pottery assigned to this group originates from Potrero-Chaquiago in Catamarca (Table 5). Given that most of this pottery can be attributed to a single site, it seems plausible that Group-3 pottery was produced at Potrero-Chaquiago. This group is chemically very homogeneous (see Figure 6) and very likely represents a single production source.

Group 4 primarily is comprised of provincial Inka pottery from Potrero de Payogasta in Salta (Tables 4 and 5); this group most likely represents pottery production in Jujuy. However, this group is somewhat heterogeneous and may include pottery from more than one production locale.

Group 5 primarily is comprised of provincial Inka and Santamariano style pottery from

Potrero-Chaquiago in Catamarca (Table 5). Given that most of this pottery can be attributed to a single site, it seems plausible that Group-3 pottery was produced at Potrero-Chaquiago. This group is chemically homogeneous (see Figure 6) and very likely represents a single production source.

Group 6 is comprised of provincial Inka pottery, most of which originates from Potrero de Payogasta in Salta (Tables 4 and 5). This group most likely represents pottery production in Jujuy. However, this group is somewhat heterogeneous and may include pottery from more than one production locale within the Salta province.

Group 7 is comprised of provincial Inka pottery, most of which originates from Yavi Chico site in Jujuy (Tables 4 and 5). This group most likely represents pottery production in Jujuy. However, this group is somewhat heterogeneous and may include pottery from more than one production locale in Jujuy.

Group 8 is a small group of pottery most of which originates from Potrero-Chaquiago in Catamarca (Tables 4 and 5). Although most of the pottery assigned to this group originates from a single site, the group represents multiple pottery types and is somewhat heterogeneous. Additional research is needed to better define the group, but it seems likely that more than production area may be subsumed within this group.

More than 90% of the pottery assigned to **Group 9** is provincial Inka and all but one sample originates from sites in the Salta province (Tables 4 and 5)—specifically Potrero de Payogasta. Consequently, Group 9 can safely be assumed to represent pottery production in the Salta province.

As part of this project 45 **clays** from Salta, Jujuy, and Catamarca provinces were analyzed by INAA. Some comparison of the clays was made with the larger reference groups. In general, the analyzed clays were a poor match with all of the reference groups—in part because these analyses are derived from untempered raw clays that have not been refined (as would have presumably been the case in large state-controlled Inka workshops). Nonetheless, when the Northwest Argentina clays are projected against the 90% confidence ellipses for the Northern Chile, Titicaca Basin, Northwest Argentina, Group X, and Group Y compositional most of the clays plot within the Northwest Argentina ellipse.

Table 6 lists membership probabilities for the clays. None of the clays exceed 1% probability of membership in Groups 1, 2, 3, 5, or 6 indicating that that clay are a poor match with these groups. Many of the clays have inflated probabilities of membership in Group-X. However, none of these clays plots consistently with group in elemental or PCA space. It is probable that the higher probabilities result from the small number of samples assigned to this group and the group's heterogeneous nature.

As discussed above, Group 4 is assumed to represent pottery production with in the Salta province specifically the site of Potrero de Payogasta. Three clays from this site are a good match with this group (Table 6). However, four clays from La Quiaca and Yavi Chico also are a

good match with this group. This is somewhat problematic. We are unfamiliar with the locations of these sites and the distances between them. Consequently, we are unable to offer much explanation for these apparently inflated probabilities. One possibility is that the clays from Jujuy and Potrero de Payogasta are derived from compositionally similar parent materials or from a common alluvial system. Alternatively, Group 4 may in fact encompass two or more compositional groups that are difficult to tease apart due to the current NAA sample. Additional samples from Jujuy and Potrero de Payogasta may aid in better understanding this phenomena.

Conclusion

This project has been successful in identifying compositional groups that can be tied to specific geographic regions within the southern Andes. Despite the fact that the analyzed sample is heavily biased toward the Catamarca province of Argentina, considerable LONG-DISTANCE trade of pottery is evident (Tables 4 and 5). Future research should focus on refinement of the Jujuy group(s?) and the Northern Chile group(s?). Such research will undoubtedly lead to a better understanding of Inka pottery production and distribution in the Southern Andes. We also suggest that future research include a petrographic component to determine if a combined mineralogical and chemical approach can provide better resolution than what we have shown here given that studies of sand, rock, and volcanic tempers may yield insights that the INAA analysis could not provide.

Acknowledgments

We acknowledge Jonathon Dake, Mark Hammond, Nicole Little, and Tessa Schut for their role in preparing the samples for irradiation. This project was supported in part by NSF grant BCS-0504015 to the Archaeometry Laboratory of the Research Reactor, University of Missouri.

References Cited

Baxter, Michael J.
1992 Archaeological uses of the biplot—a neglected technique? In *Computer Applications and Quantitative Methods in Archaeology, 1991*, edited by G. Lock and J. Moffett. BAR International Series S577, 141–148. Tempvs Reparatvm, Archaeological and Historical Associates, Oxford.
1994a *Exploratory Multivariate Analysis in Archaeology*. Edinburgh University Press, Edinburgh.
1994b Stepwise discriminant analysis in archaeometry: a critique. *Journal of Archaeological Science* 21:659–666.

Bieber, Alan M. Jr., Dorothea W. Brooks, Garman Harbottle, and Edward V. Sayre
1976 Application of multivariate techniques to analytical data on Aegean ceramics. *Archaeometry* 18:59–74.

Bishop, Ronald L. and Hector Neff
1989 Compositional data analysis in archaeology. In *Archaeological Chemistry IV*, edited by R. O. Allen, pp. 576–586. Advances in Chemistry Series 220, American Chemical Society, Washington, D.C.

Bishop, Ronald L., Robert L. Rands, and George R. Holley
1982 Ceramic compositional analysis in archaeological perspective. In *Advances in Archaeological Method and Theory*, vol. 5, pp. 275–330. Academic Press, New York.

Glascock, Michael D.
1992 Characterization of archaeological ceramics at MURR by neutron activation analysis and multivariate statistics. In *Chemical Characterization of Ceramic Pastes in Archaeology*, edited by H. Neff, pp. 11–26. Prehistory Press, Madison, WI.

Harbottle, Garman
1976 Activation analysis in archaeology. *Radiochemistry* 3:33–72. The Chemical Society, London.

Leese, Morven N. and Peter L. Main
1994 The efficient computation of unbiased Mahalanobis distances and their interpretation in archaeometry. *Archaeometry* 36:307–316.

Loose, Richard W.
1977 Petrographic notes on selected lithic and ceramic materials. In *Settlement and Subsistence Along the Lower Chaco River*, edited by C. Reher, pp. 567–571. University of New Mexico Press, Albuquerque.

Lynott, Mark J., Hector Neff, James E. Price, James W. Cogswell, and Michael D. Glascock
2000 Inferences about prehistoric ceramics and people in Southeast Missouri: Results of ceramic compositional analysis. American Antiquity, 65(1): 103–126.

Neff, Hector
1992 Introduction. In *Chemical Characterization of Ceramic Pastes in Archaeology*, edited by H. Neff, pp. 1–10. Prehistory Press, Madison, WI.
1994 RQ-mode principal components analysis of ceramic compositional data. *Archaeometry* 36:115–130.
2000 Neutron activation analysis for provenance determination in archaeology. In *Modern Analytical Methods in Art and Archaeology*, edited by E. Ciliberto and G. Spoto, pp. 81–134. John Wiley and Sons, Inc., New York.
2002 Quantitative techniques for analyzing ceramic compositional data. In Ceramic *Source Determination in the Greater Southwest*, edited by D. M. Glowacki and H. Neff. Monograph 44, Cotsen Institute of Archaeology, UCLA, Los Angeles.

Neff, Hector, Jeffrey Blomster, Michael D. Glascock, Ronald D. Bishop, M. James Blackman, Michael D. Coe, George L. Cowgill, Richard A. Diehl, Stephen Houston, Artur A. Joyce, Carl P. Lipo, Barbara L. Stark, and Marcus Winter
2006 Methodological Issues in the Provenance Investigation of Early Formative Mesoamerican Ceramics. *Latin American Antiquity,* In review.

Rautman, Marcus L., Basil Gomez, Hector Neff, and Michael D. Glascock
1993 Neutron Activation Analysis of Late Roman Ceramics from Kalavasos-Kopetra and the Environs of the Vasilikos Valley. In *Report of the Department of Antiquities, Cyprus 1993*. Pp. 233–265.

Robinson, David G.
2004 Petrographis Analysis of Prehistoric Ceramics from two sites in La Junta Archaeological District, Presidio County, Trans-Pecos, Texas. In The Arroyo de la Presa Site: A Stratified Late Prehistoric Campsite Along the Rio Grande, Presidio County, Trans-Pecos Texas. Reports in Contract Archaeology 9. Center for Big Bend Studies, Sul Ross State University, Texas.

Sayre, Edward V.
1975 Brookhaven Procedures for Statistical Analyses of Multivariate Archaeometric Data. Brookhaven National Laboratory Report BNL-23128. New York.

Steponaitis, Vincas, M. James Blackman, and Hector Neff
1996 Large-scale compositional patterns in the chemical composition of Mississippian pottery. *American Antiquity* 61:555–572.

Weigand, Phil C., Garman Harbottle, and Edward V. Sayre
1977 Turquoise sources and source analysis: Mesoamerica and the southwestern U.S.A. In *Exchange Systems in Prehistory*, edited by T. K. Earle and J. E. Ericson, pp. 15–34. Academic Press, New York.

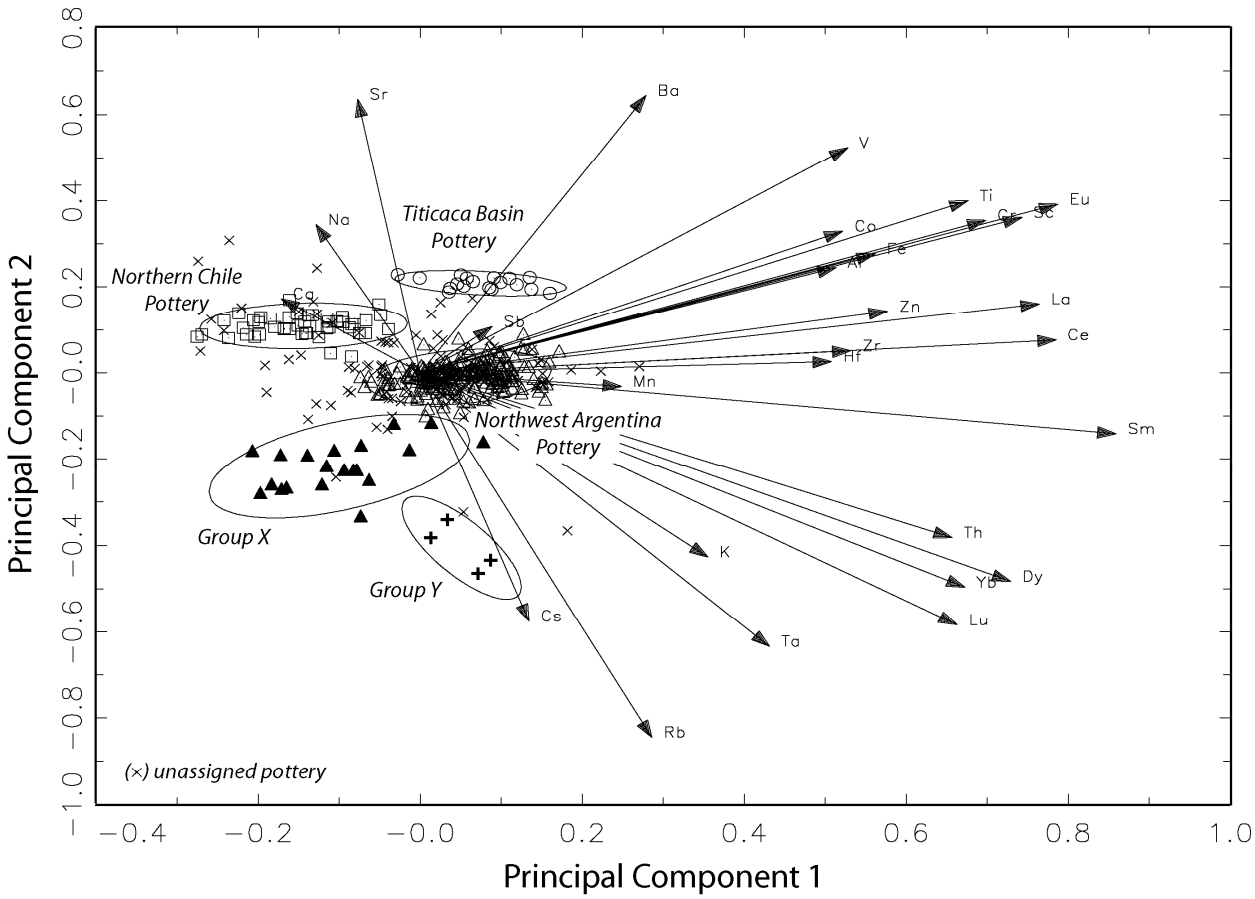

Figure 1. Correlation-matrix biplot of principal component 1 and 2 based on PCA of the Inka pottery dataset. Ellipses represent the 90% confidence interval for group membership.

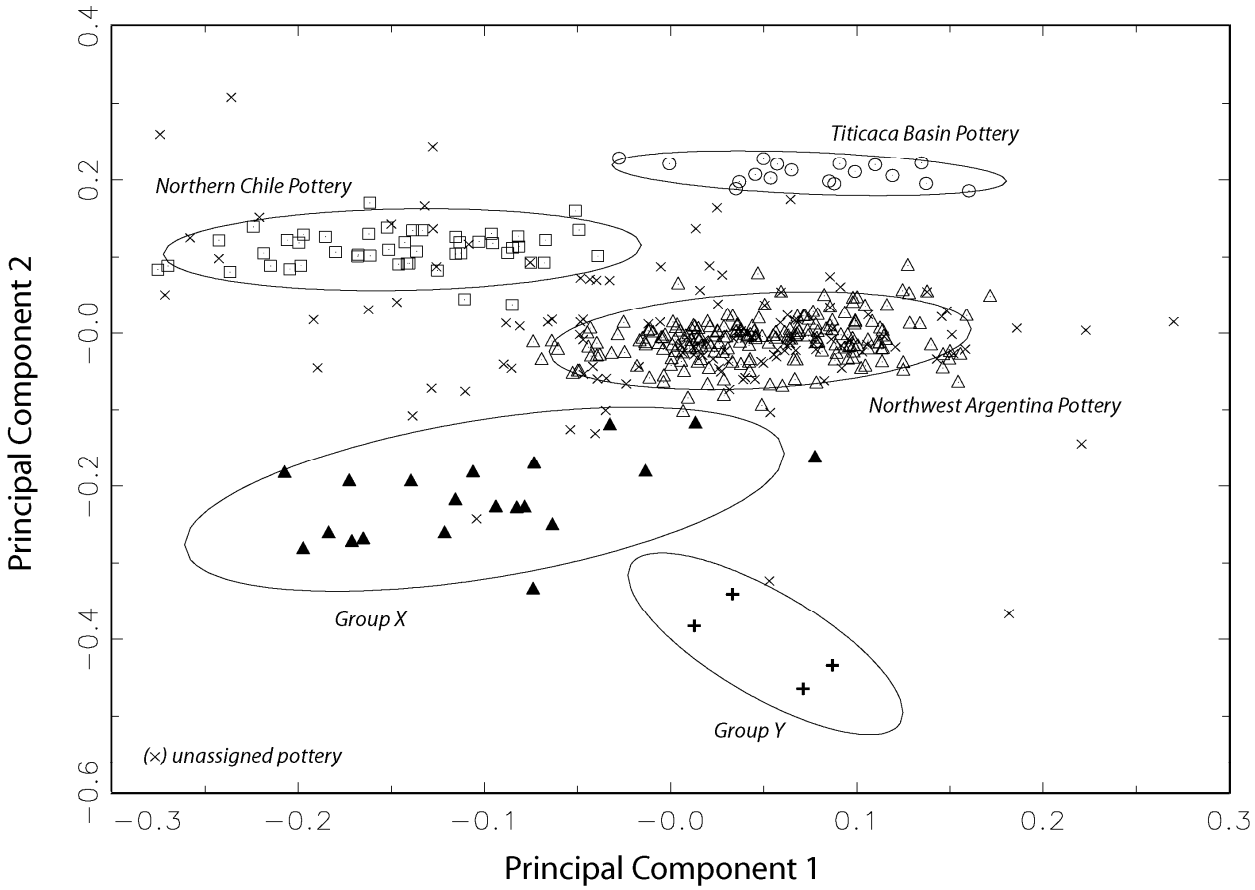

Figure 2. Correlation-matrix plot of principal component 1 and 2 based on PCA of the Inka pottery dataset. Ellipses represent the 90% confidence interval for group membership. *Same as Figure 1, but without vectors.*

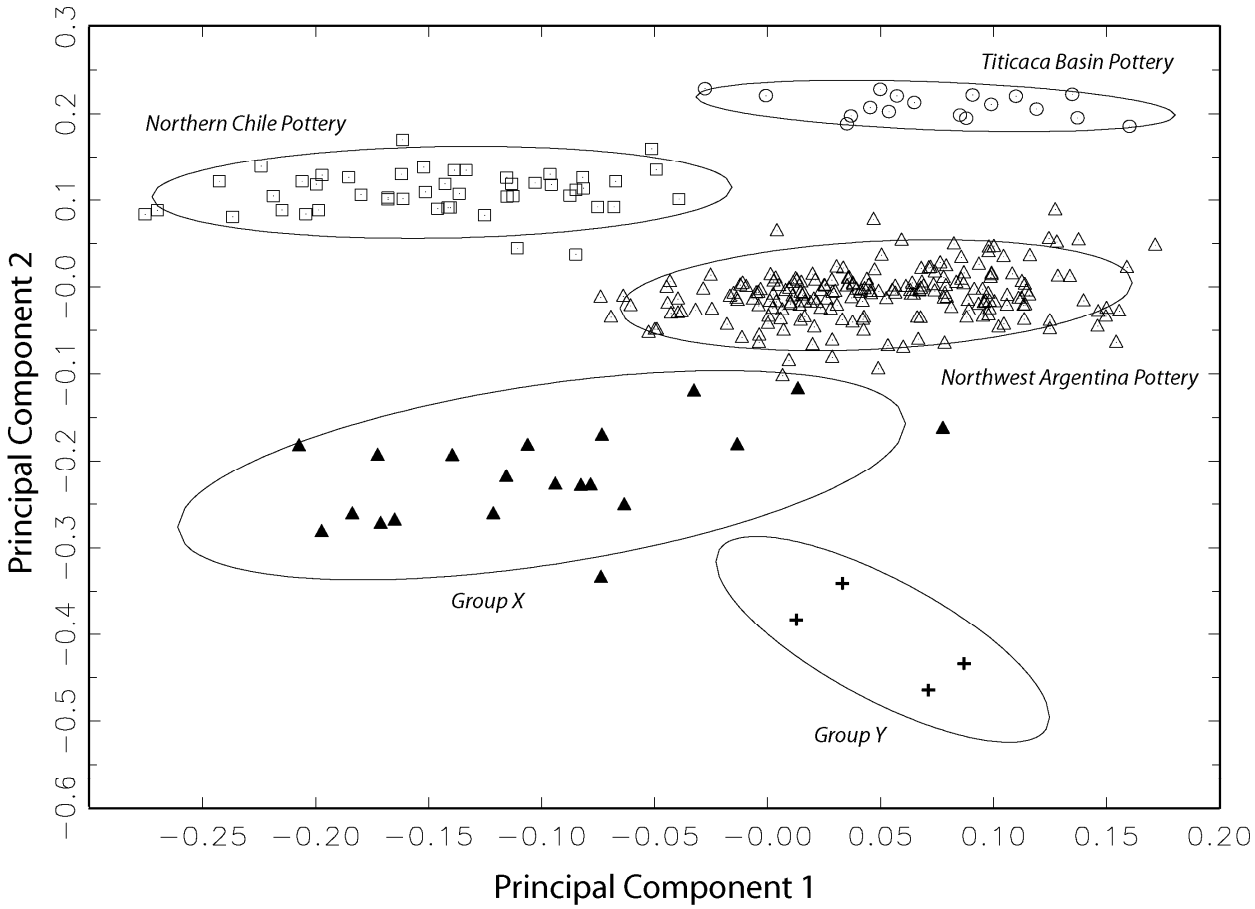

Figure 3. Correlation-matrix plot of principal component 1 and 2 based on PCA of the Inka pottery dataset. Ellipses represent the 90% confidence interval for group membership. *Same as Figure 2, but without unassigned samples.*

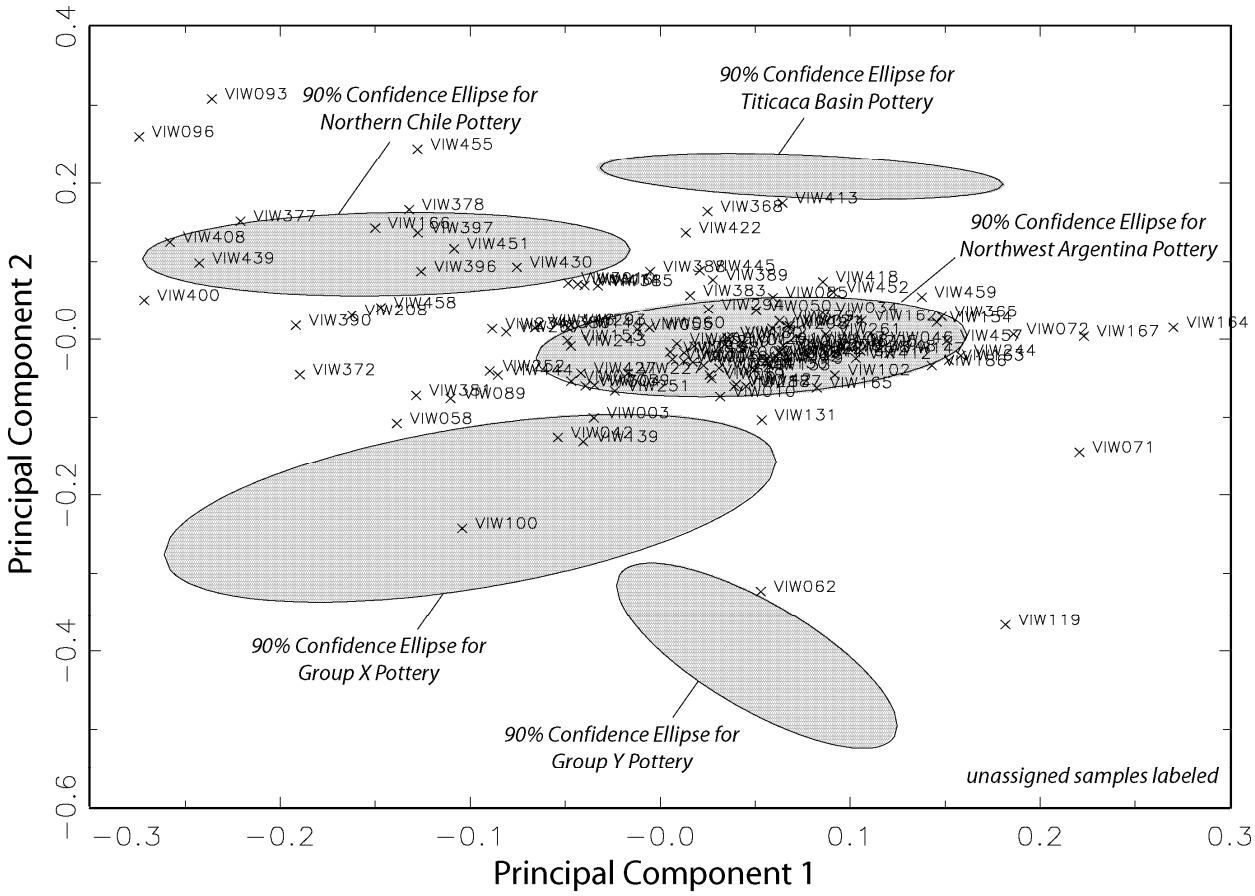

Figure 4. Correlation-matrix plot of principal component 1 and 2 based on PCA of the Inka pottery dataset with unassigned specimens projected against 90% confidence ellipses for the groups.

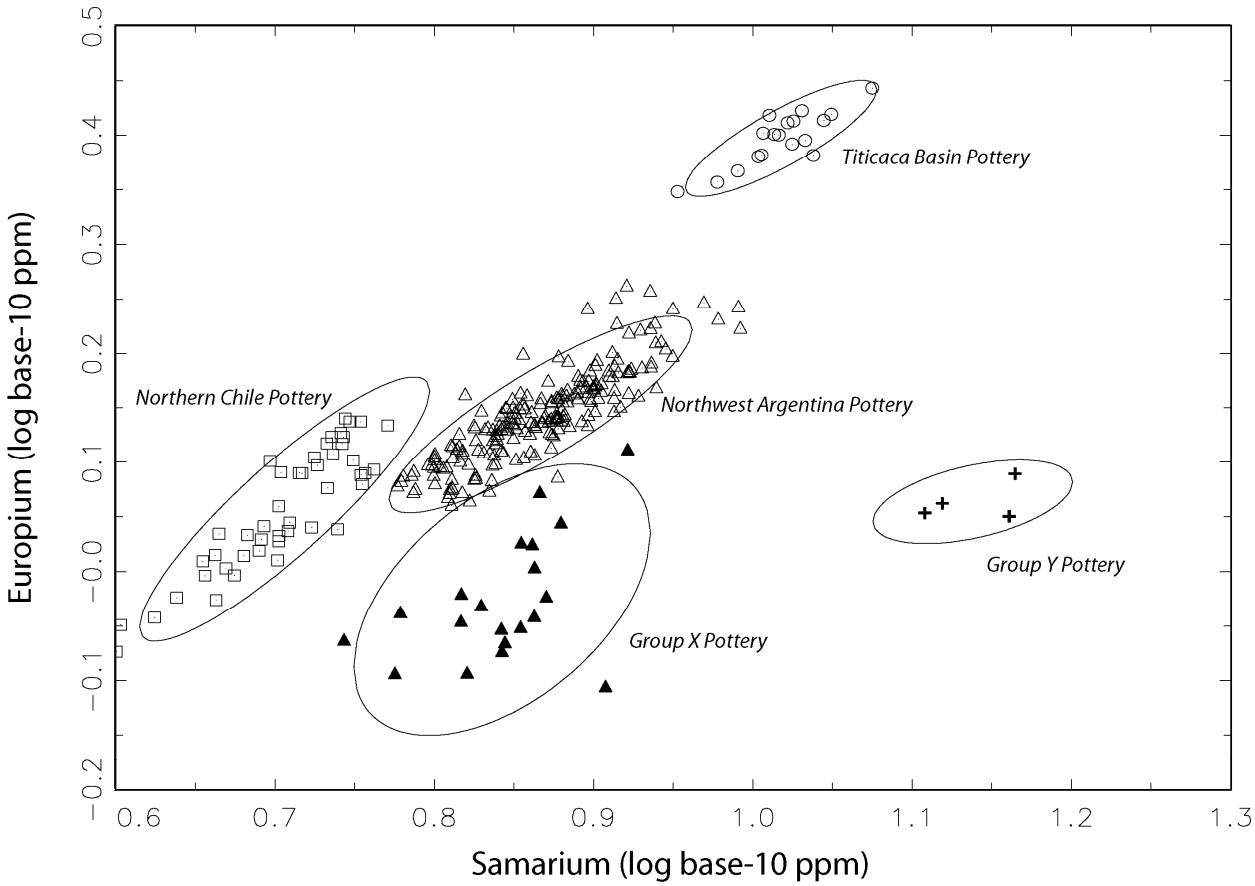

Figure 5. Plot of samarium and europium base-10 logged concentrations for pottery from Northern Chile, the Titicaca Basin, Northwest Argentina, and two unknown production areas (Group X and Group Y). Ellipses represent the 90% confidence interval for group membership.

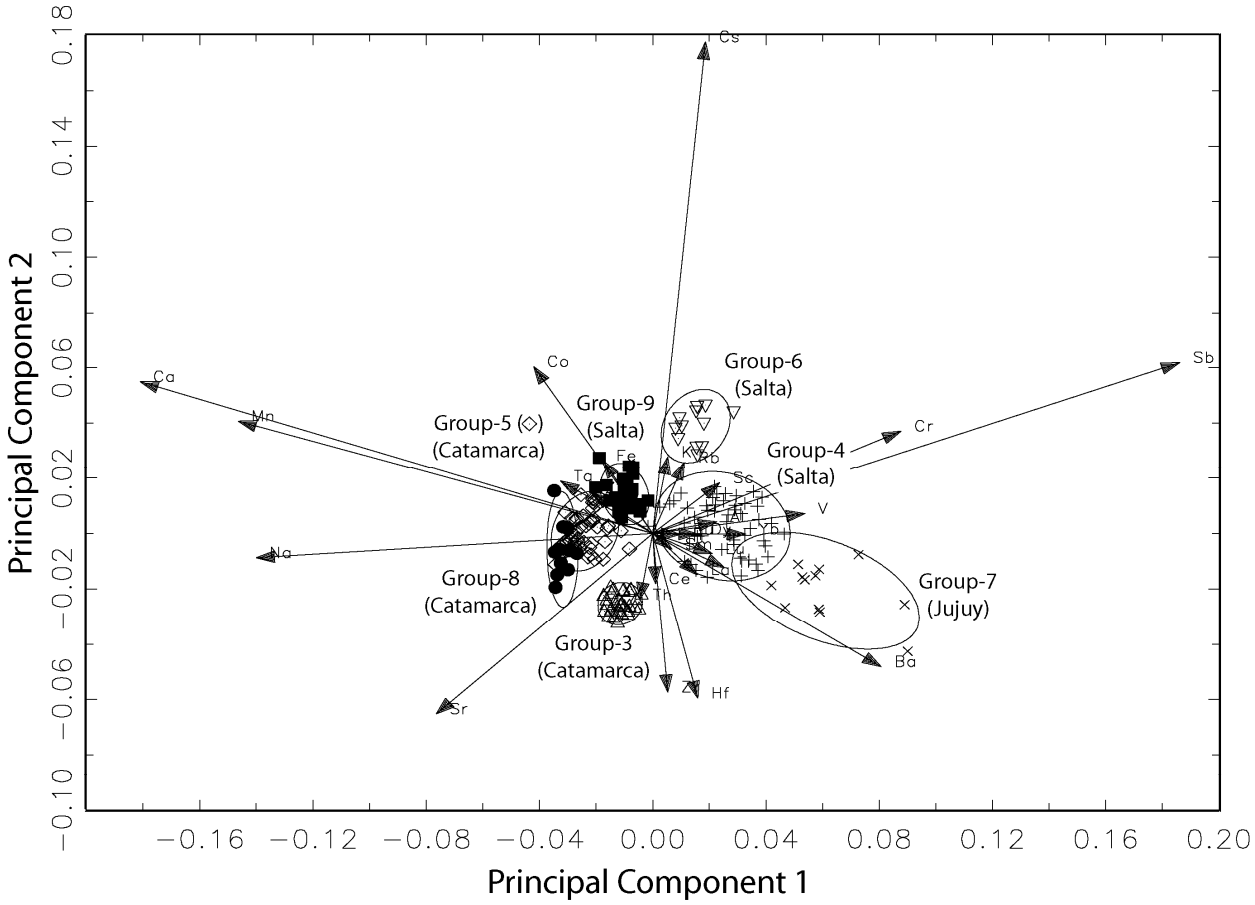

Figure 6. Variance-covariance matrix biplot of principal component 1 and 2 based on PCA of the Northwest Argentina pottery group (see Figures 1–5). Ellipses represent the 90% confidence interval for group membership.

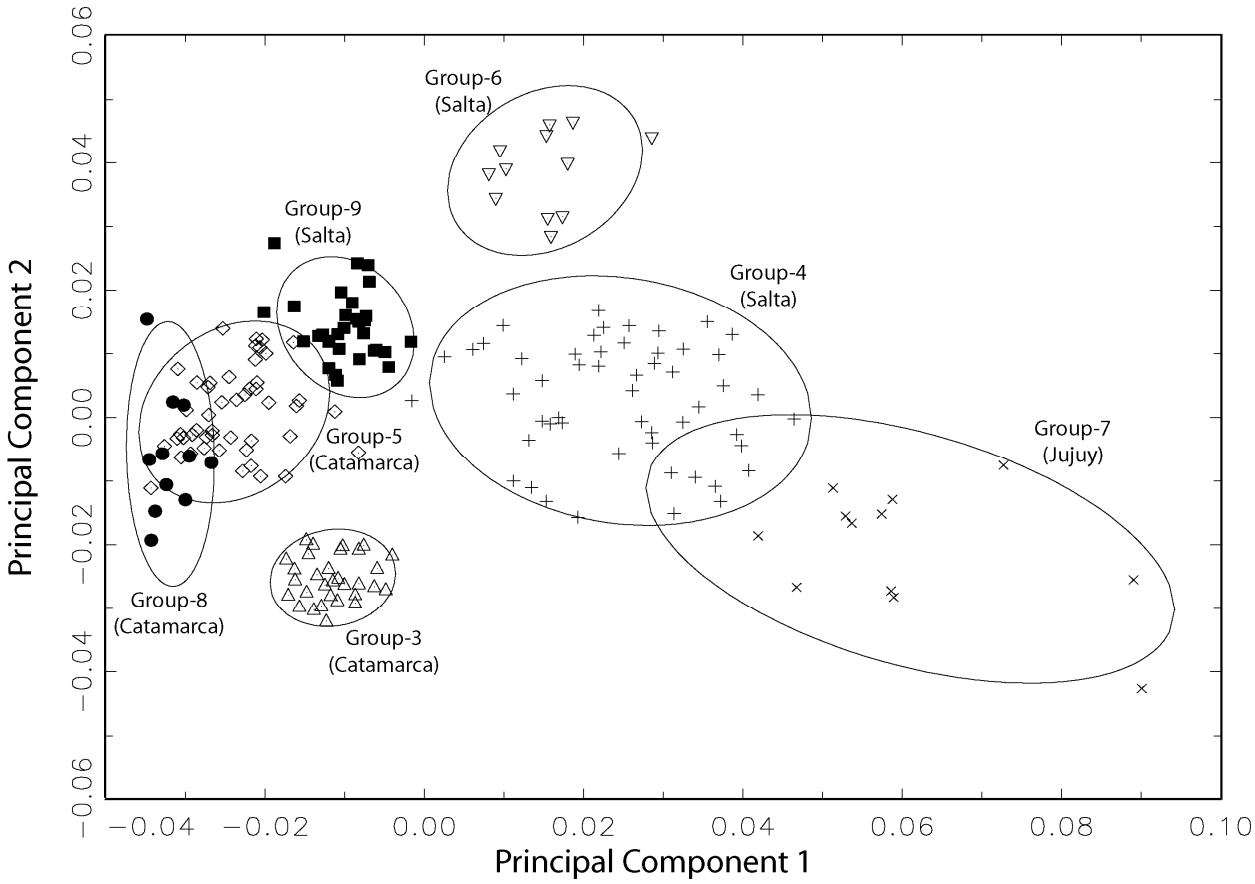

Figure 7. Variance-covariance matrix plot of principal component 1 and 2 based on PCA of the Northwest Argentina pottery group (see Figures 1–5). Ellipses represent the 90% confidence interval for group membership. *Same as Figure 6, but without the vectors.*

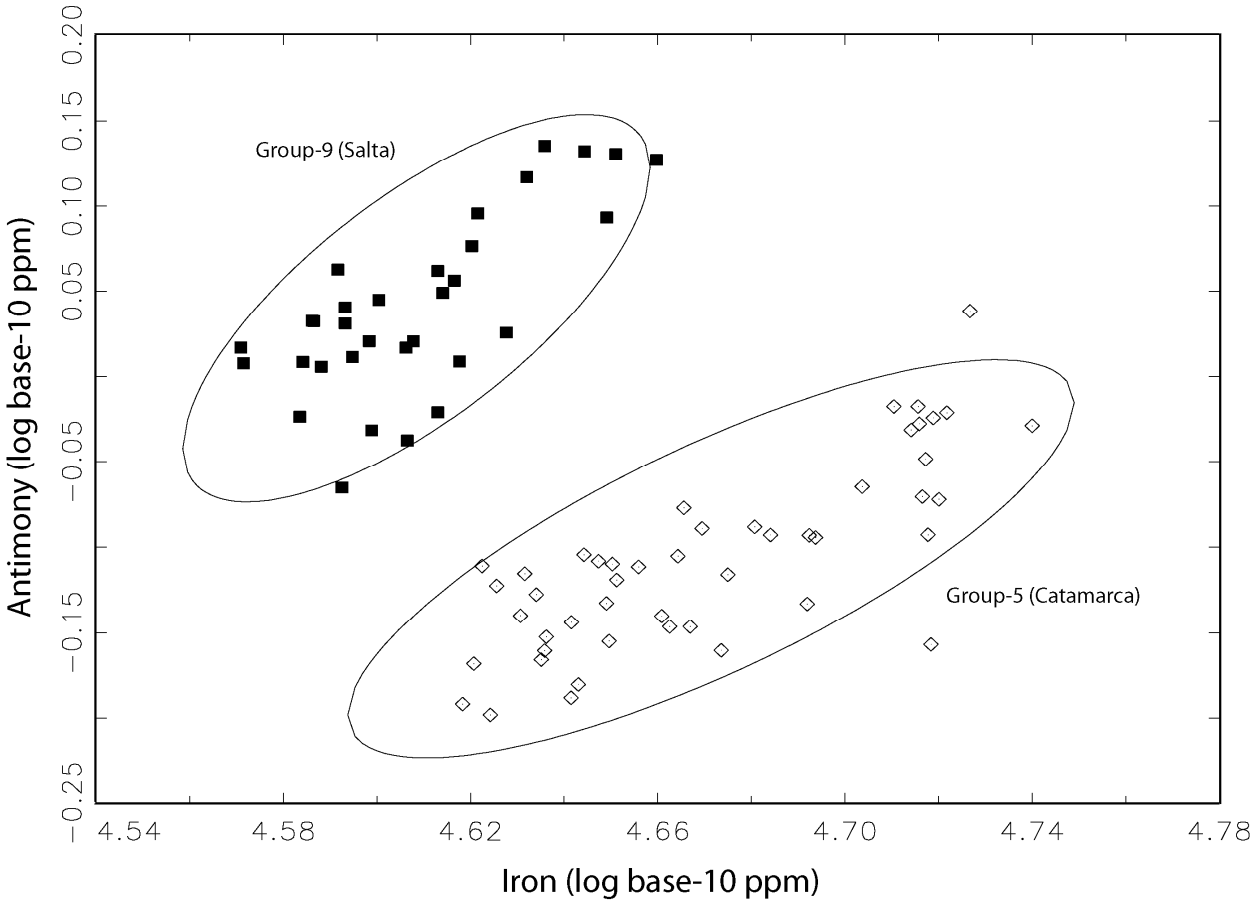

Figure 8. Plot of iron and antimony base-10 logged concentrations showing separation of Groups 5 and 9. Ellipses represent the 90% confidence interval for group membership.

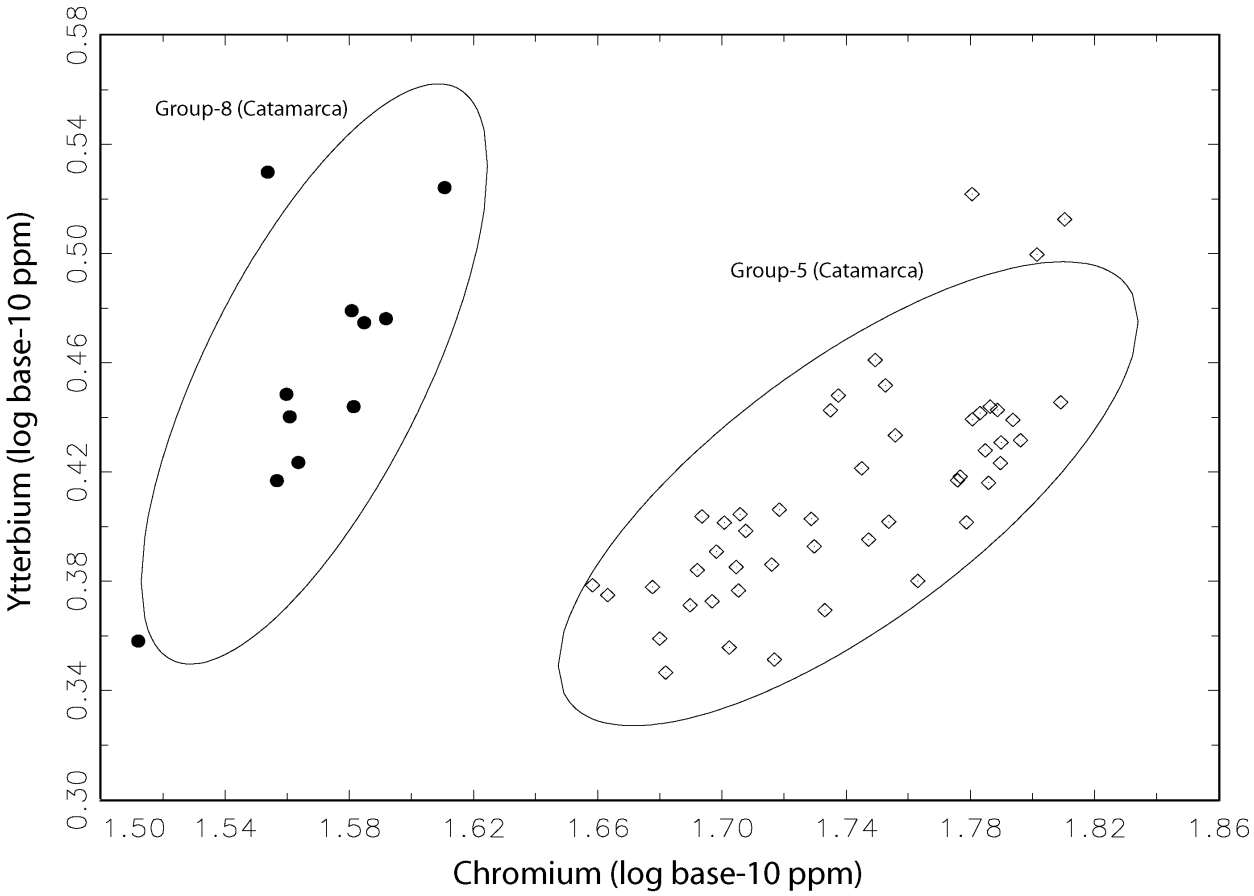

Figure 9. Plot of chromium and ytterbium base-10 logged concentrations showing separation of Groups 5 and 8. Ellipses represent the 90% confidence interval for group membership.

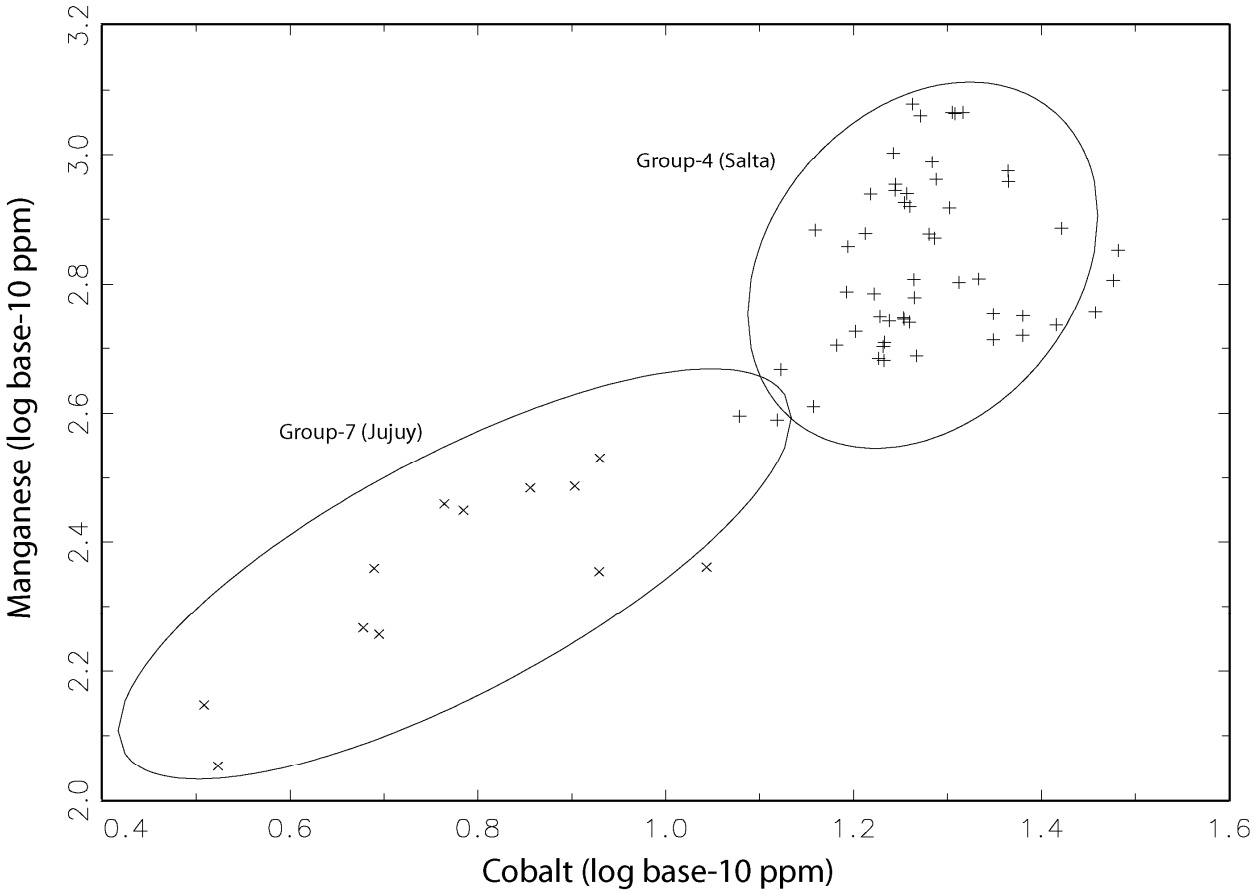

Figure 10. Plot of iron and antimony base-10 logged concentrations showing separation of Groups 4 and 7. Ellipses represent the 90% confidence interval for group membership.

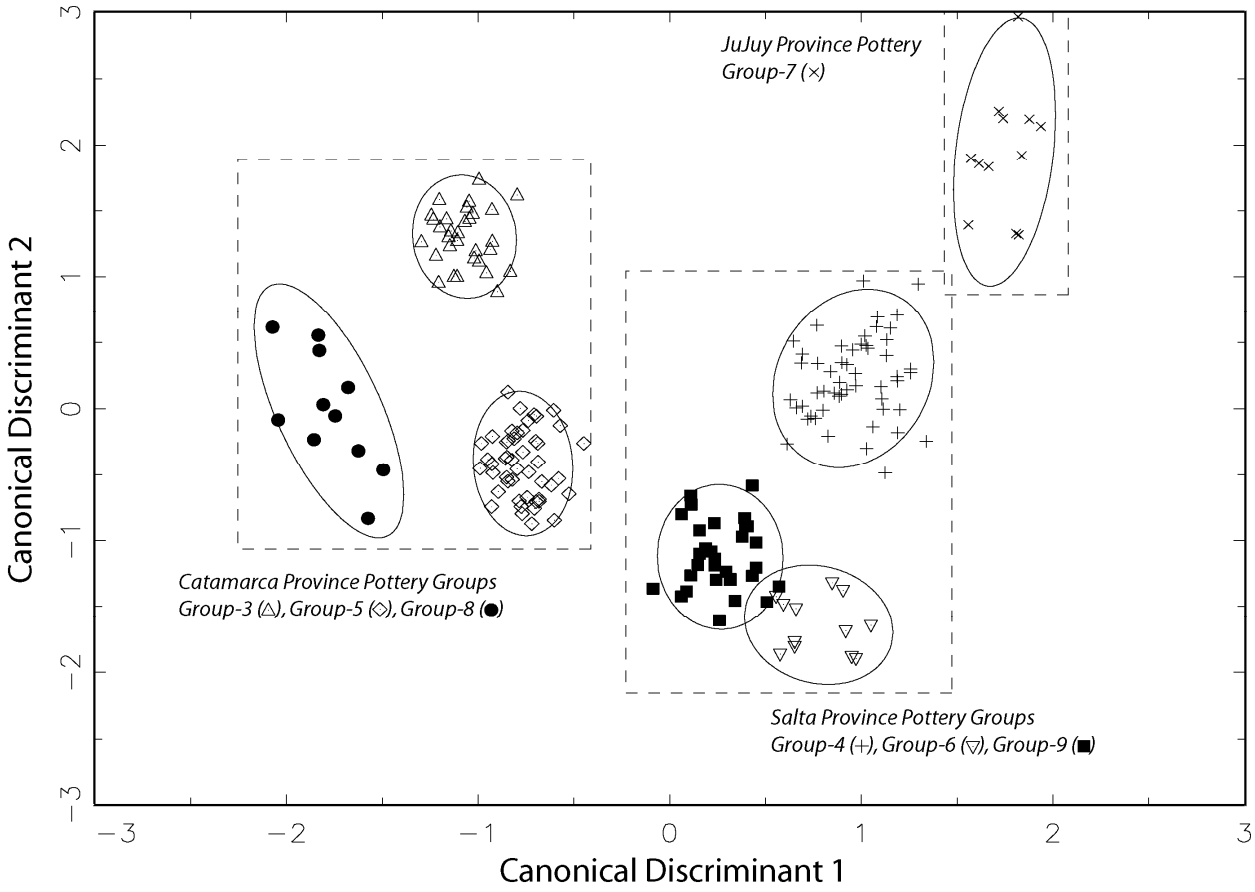

Figure 11. Discriminant analysis plot showing separation of all Northwest Argentina pottery groups. Ellipses represent the 90% confidence interval for group membership.

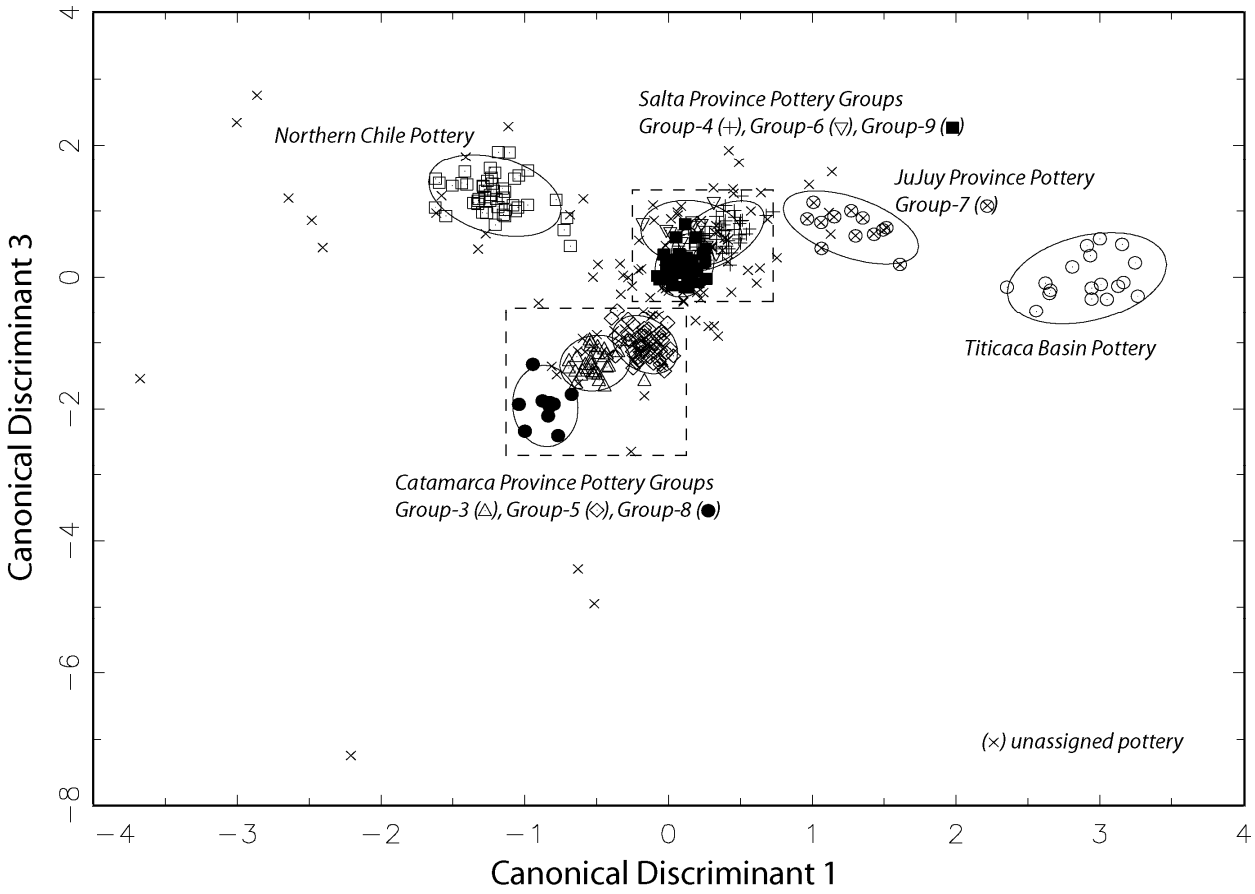

Figure 12. Discriminant analysis plot showing separation Northwest Argentina pottery groups from pottery produced in Northern Chile and the Titicaca Basin. Ellipses represent the 90% confidence interval for group membership.

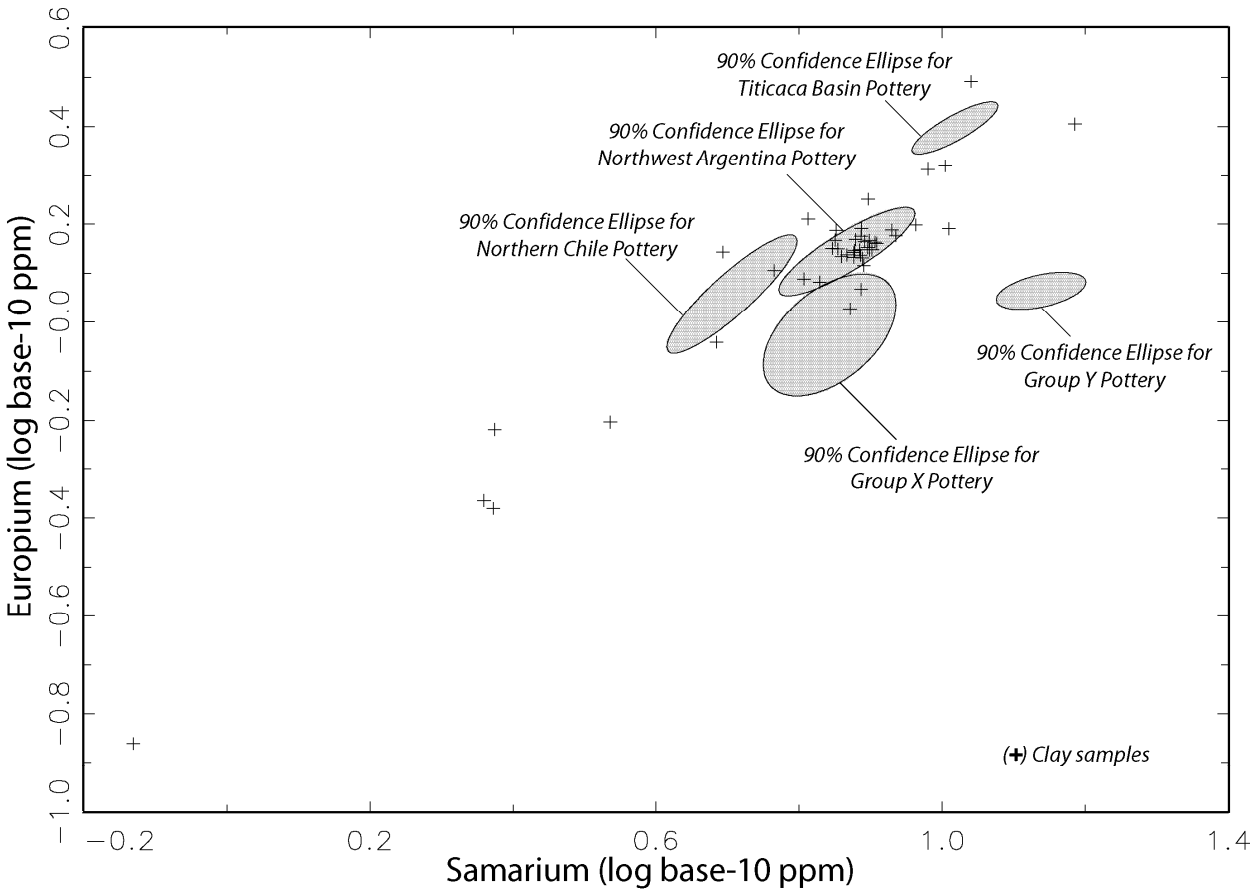

Figure 13. Plot of samarium and europium base-10 logged concentrations in which clay samples are projected against 90% confidence ellipses calculated for the Northern Chile, Titicaca Basin, Northwest Argentina, Group X, and Group Y compositional groups.

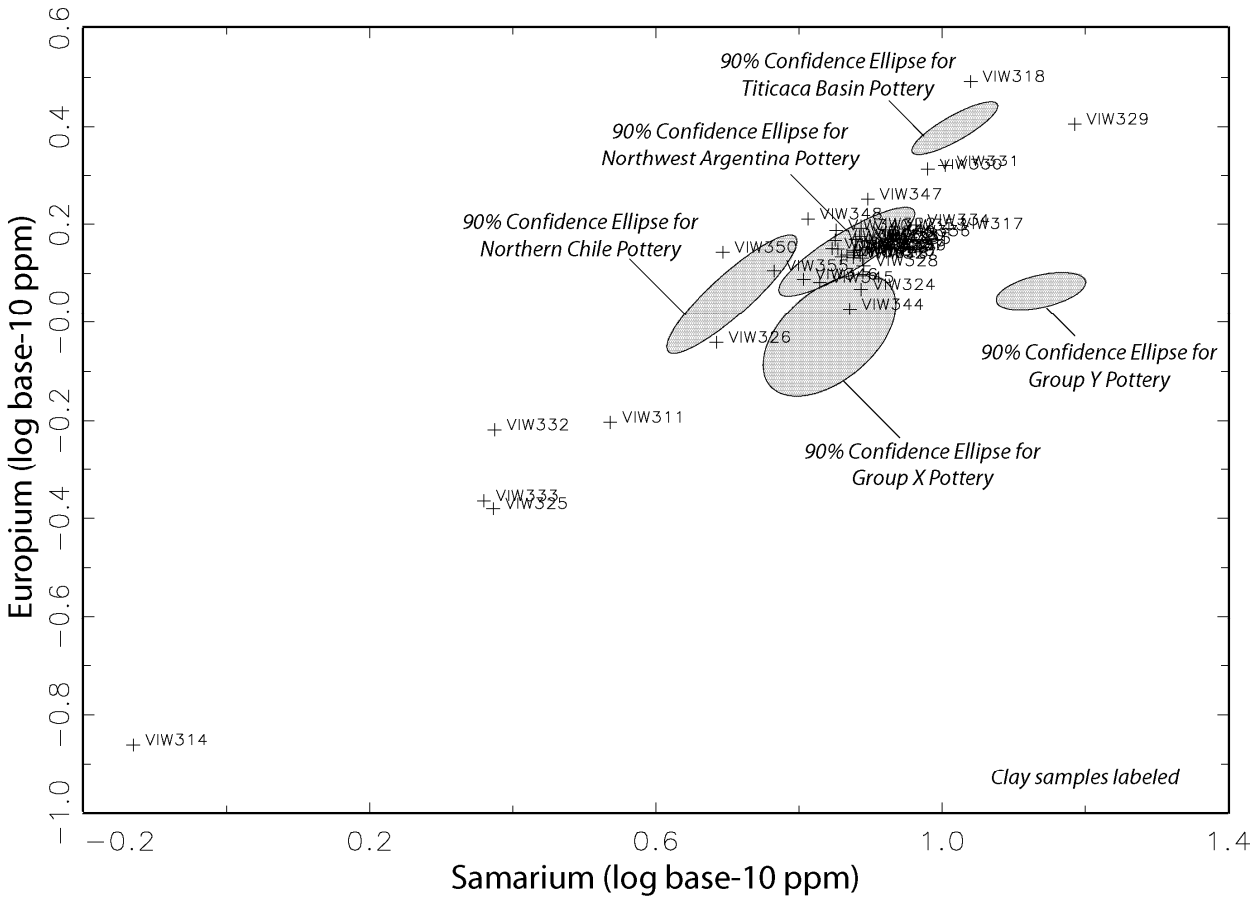

Figure 14. Plot of samarium and europium base-10 logged concentrations in which clay samples are projected against 90% confidence ellipses calculated for the Northern Chile, Titicaca Basin, Northwest Argentina, Group X, and Group Y compositional groups. *Same as Figure 13, but with unassigned samples labeled.*